Direct Adaptive Rejection of Narrow-Band Disturbances Based on Youla-Kucera Parameterization

Qixing Zheng and Masayoshi Tomizuka

Department of Mechanical Engineering

University of California at Berkeley, Berkeley, California 94720, U.S.A.

qiz@me.berkeley.edu, tomizuka@me.berkeley.edu

Abstract

This report presents a method to handle narrow-band disturbances in hard disk drives (HDDs) by modifying the baseline servo controller. A direct adaptive controller with Q filter is built around the baseline servo controller to reject the narrow-band disturbances based on Youla-Kucera parameterization. The coefficients of the Q filter are updated in such a way that the resulting controller incorporates the internal model of the narrow-band disturbances. Two modifications are made in the direct adaptive control in this report: one is adding a pre-specified term to the Q filter to avoid large transient oscillation; the other is cascading the Q filter with a bandpass filter to limit the waterbed effect to a certain frequency range. The performance of the proposed servo controller is demonstrated by simulation on an open-source HDD benchmark problem.

Keywords: Direct adaptive control, hard disk drives, internal model principle, narrow-band disturbance, Youla-Kucera parameterization.

1. Introduction

One of the most important issues in the track following control of hard disk drives (HDDs) is to keep the track mis-registration (TMR) small. TMR is defined as three times the standard deviation of the position error signal (PES) which is proportional to the radial distance between the position of the read/write head and the reference track center. The source of TMR is the disturbances in HDD, including repeatable runout (RRO) and non-repeatable runout (NRRO).

Narrow-band disturbances contribute a lot to both the repeatable and the non-repeatable runouts, but the narrow-band disturbances in these two runouts are different in nature. The RRO is locked to the spindle rotation in both frequency and phase, which makes the frequency and phase of the narrow-band disturbances in the RRO time-invariant. The RRO can be rejected either by improving the precision of the servo-writer during the manufacturing processes or by servo control algorithms such as repetitive control [1] and adaptive feedforward control [2]. Unlike the RRO, the NRRO contains narrow-band signals with time-varying phases and magnitudes at unknown frequencies. The NRRO can be rejected by improving the mechanical design: e.g. an improved spindle motor using damping material [3]. However this time-consuming re-design of a mechanical component will significantly increase the cost of disk drives. So it is preferable to handle the narrow-band disturbances in the NRRO by the servo algorithm.

The traditional servo methods of rejecting narrow-band disturbances in the NRRO include different kinds of peak filters [4][5][6]. The difficulty of determining the center frequency of the peak filters remains for these methods. One way to effectively compensate for the narrow-band disturbances with unknown or time-varying frequency is adaptive control. The block diagram of a typical

adaptive control system for HDDs is shown in Fig. 1. This system first identifies the disturbance model (the frequency estimator in Fig. 1 for the narrow-band disturbance case). Based on the identified disturbance model (the identified frequency), a disturbance compensator, which can be a peak filter [7] or the basis function algorithm [8], is adjusted to reject the disturbance. The adaptation of the compensator is indirect via the frequency estimator, and this approach is called *indirect adaptive control*. The main drawback of this indirect adaptive control scheme is the long convergence time required for frequency identification. From the simulation result of frequency identification for a narrow-band disturbance at 600Hz shown in Fig. 2, we can see that the convergence takes about one revolution (220 samples), which means that no compensation can be achieved within the first revolution after the indirect adaptive controller is activated. The other method to adapt the compensator is direct adaptive control, which integrates the identifier and the compensator into one adaptive algorithm. In this report, we introduce a direct adaptive control scheme to achieve fast attenuation of narrow-band disturbances in HDD systems.

Landau, Constantinescu, and Rey applied both direct and indirect adaptive control to an active suspension to reject external vibrations. The authors showed by real time experiments that direct adaptive control provided more attenuation than indirect adaptive control. They also reported two problems associated with direct adaptive control: the large adaptation transients and the influence of inaccurate plant models.

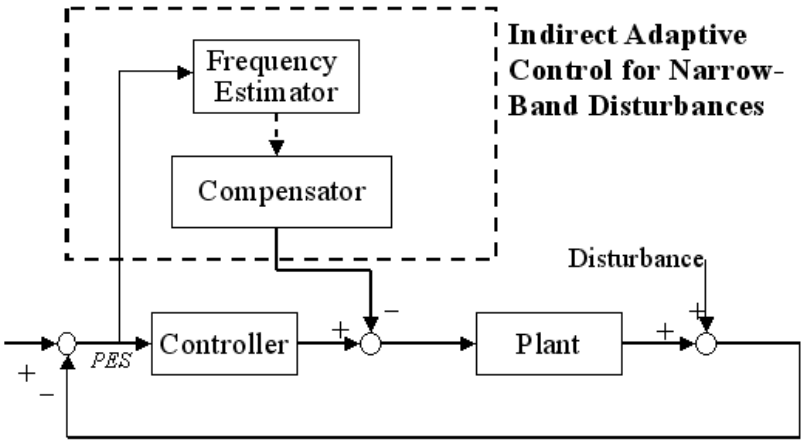

Fig. 1. Structure of an indirect adaptive control scheme for rejecting narrow-band disturbances.

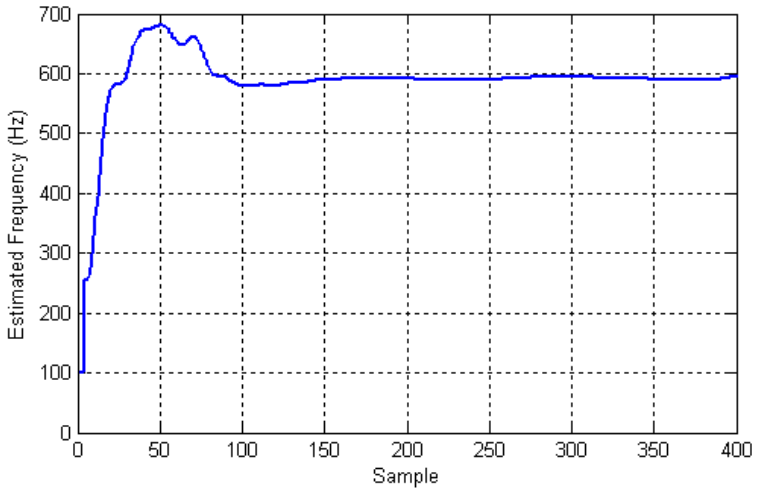

Fig. 2. Simulation result of frequency identification for indirect adaptive control.

In this report, we use a direct adaptive servo controller to reject narrow-band disturbances in HDD systems based on Youla-Kucera parameterization. The structure of this controller is shown in Fig. 3. Only the track following control for HDD is considered in this report, i.e. the reference signal for feedback control is zero. $G(z^{-1})$ represents the hard disk drive system, including the power amplifier, the voice coil motor (VCM), and the head stack assembly (HSA). The baseline servo controller is a PID controller (given by $R_0(z^{-1})/S_0(z^{-1})$) cascaded with notch filters tuned not to excite the resonant modes. For the simplicity of the adaptive controller design, $G(z^{-1})$ together with the notch

filters are considered as the plant of the system, which is denoted by $P(z^{-1})$. The HDD system is affected by the disturbance d, which includes RRO, sensor noise, disk flutters, external vibration, etc. $z^{-d}B(z^{-1})/A(z^{-1})$ is the discrete-time transfer function of the plant model, a simplified approximation of the plant $P(z^{-1})$. The signal w is applied to an adaptation algorithm to adjust the parameters of the finite-impulse-response Q filter, $\hat{Q}(z^{-1})$. The adaptation algorithm is designed based on the internal model principle to achieve asymptotic rejection of narrow-band disturbances.

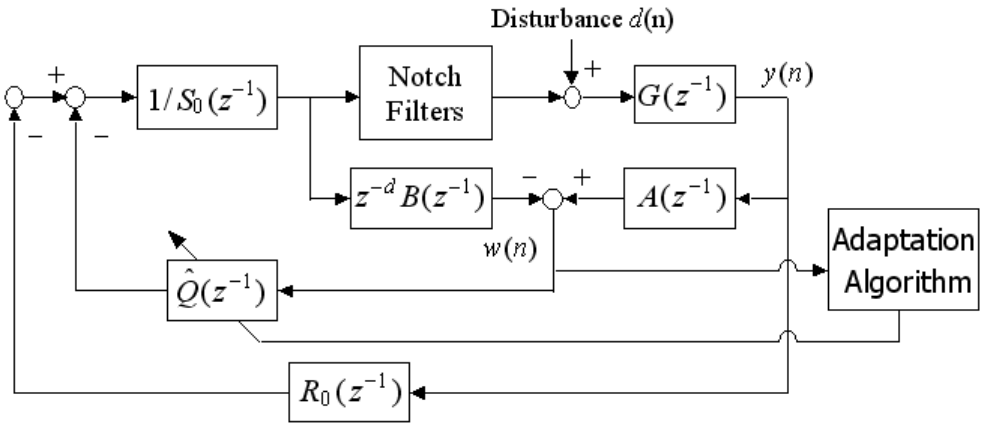

Fig. 3. Structure of the direct adaptive control scheme.

The remainder of this report is organized as follows. In Section 2, we will give more details of the plant, the plant model and the baseline servo controller as well as a review of the Youla-Kucera parameterization and the internal model principle. Section 3 is dedicated to describing the adaptation algorithm similar to the one presented in [9] for rejecting narrow-band disturbances. Simulation results of the direct adaptive controller are shown in Section 4. Two modifications to the direct adaptive controller are introduced in Section 5 to improve the transient performance and to constrain the waterbed effect. The conclusion is drawn in Section 6.

2. HDD plant and baseline servo controller

The VCM actuator of an HDD system is usually modeled as a double-integrator. But the experimentally obtained frequency response of the VCM shows a 0 dB/decade slope at low frequencies due to pivot friction [10]. Therefore, in our simulation, the VCM possesses a pair of complex conjugate poles in the low frequency region. The full model of the plant is a fourteenth order transfer function with several high frequency resonance modes. This model as well as our simulation tool is taken from an open-source HDD benchmark problem [11]. Figure 4 shows the frequency response of the full order model. We can see that there are resonance modes at around 4,000Hz, 5,000Hz, and 7,000Hz.

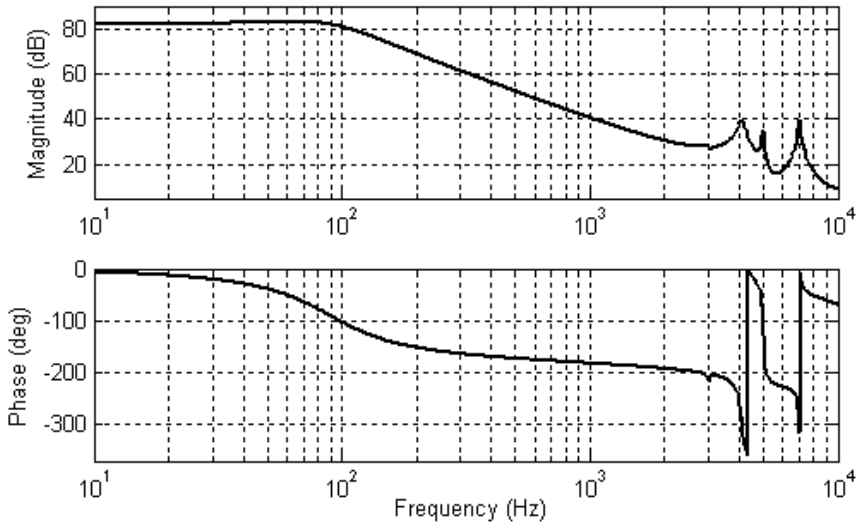

Fig. 4. Frequency response of the full model.

The baseline servo controller we use is also from [11]. Figure 5 shows the frequency response of the baseline controller, which is a second-order PID controller cascaded with notch filters tuned to compensate for the resonance modes. The transfer function of the PID controller is given by

$$C_{PID}(z^{-1}) = \frac{0.0432 - 0.0853z^{-1} + 0.0420z^{-2}}{1 - z^{-1}}. \quad (1)$$

We need a computationally simple controller and a plant model for the direct adaptive control design. So the full model of the plant and the notch filters are considered as the HDD plant, the frequency response of which is shown by the solid line in Fig. 6. This HDD plant is further simplified to a third-order plant model given by

$$P_m(z^{-1}) = \frac{z^{-2}(3.014 + 2.991z^{-1})}{1 - 1.977z^{-1} + 0.9769z^{-2}}, \tag{2}$$

the frequency response of which is represented by the dashed line in Fig. 6. As mentioned in Section 1, the baseline controller $C_{PID}(z^{-1})$ and the plant model $P_m(z^{-1})$ are denoted as

$$C_{PID}(z^{-1}) = \frac{R_0(z^{-1})}{S_0(z^{-1})}, \tag{3}$$

$$P_m(z^{-1}) = \frac{z^{-d}B(z^{-1})}{A(z^{-1})}, \tag{4}$$

where $R_0(z^{-1}) = 0.0432 - 0.0853z^{-1} + 0.0420z^{-2}$, $S_0(z^{-1}) = 1 - z^{-1}$, $B(z^{-1}) = 3.014 + 2.991z^{-1}$, $A(z^{-1}) = 1 - 1.977z^{-1} + 0.9769z^{-2}$, and $d = 2$.

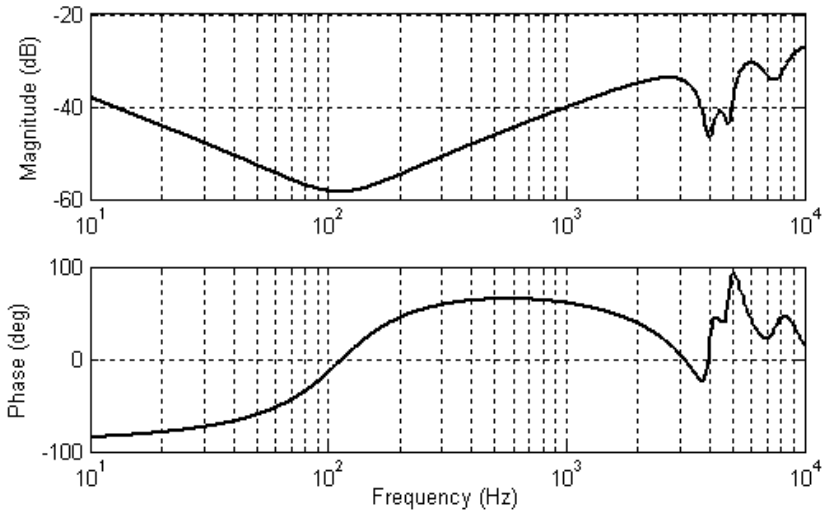

Fig. 5. Frequency response of the baseline controller.

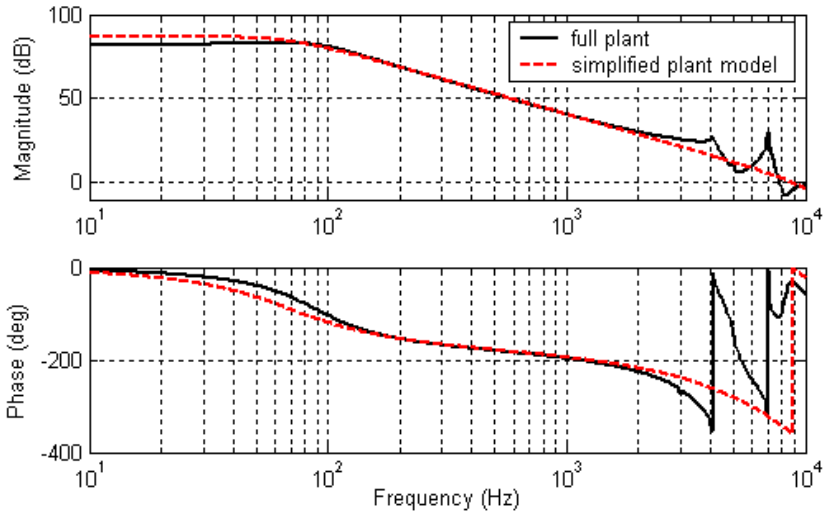

Fig. 6. Frequency response of the plant and the plant model.

Suppose that the HDD plant is identical to our plant model. Then, the resulting closed-loop polynomial is

$$H(z^{-1}) = A(z^{-1})S_0(z^{-1}) + z^{-d}B(z^{-1})R_0(z^{-1}). \tag{5}$$

Since the closed-loop system with the baseline controller is stable, all the roots of the closed-loop polynomial are stable or inside the unit circle. One useful methodology of designing controllers is the Youla-Kucera parameterization, which states that all stabilizing controllers for the plant $z^{-d}B(z^{-1})/A(z^{-1})$ have the form $R(z^{-1})/S(z^{-1})$, where

$$R(z^{-1}) = R_0(z^{-1}) + A(z^{-1})Q(z^{-1}), \tag{6}$$

$$S(z^{-1}) = S_0(z^{-1}) - z^{-d}B(z^{-1})Q(z^{-1}). \tag{7}$$

$Q(z^{-1})$ is a polynomial of z^{-1} with order n_Q:

$$Q(z^{-1}) = q_0 + q_1 z^{-1} + \cdots + q_{n_Q} z^{-n_Q}. \tag{8}$$

Note that the resulting closed-loop polynomial remains the same for all the stabilizing controllers:

$$
\begin{aligned}
&A(z^{-1})S(z^{-1}) + z^{-d}B(z^{-1})R(z^{-1}) \\
&= A(z^{-1})S_0(z^{-1}) - z^{-d}A(z^{-1})B(z^{-1})Q(z^{-1}) + z^{-d}B(z^{-1})R_0(z^{-1}) + z^{-d}A(z^{-1})B(z^{-1})Q(z^{-1}) \\
&= A(z^{-1})S_0(z^{-1}) + z^{-d}B(z^{-1})R_0(z^{-1})
\end{aligned} \tag{9}
$$

The controller $R(z^{-1})/S(z^{-1})$ can be implemented as shown in Fig. 3. In the figure, the adaptation algorithm is not included and the Q filter is fixed. The Q filter gives us extra flexibility to tune the controller without sacrificing the stability.

The narrow-band disturbance is modeled as a sinusoidal signal. The Z transform of a sinusoidal signal is given by

$$
D(z^{-1}) = \frac{B_d(z^{-1})}{A_d(z^{-1})}, \tag{10}
$$

where $A_d(z^{-1}) = 1 - 2\cos(\omega)z^{-1} + z^{-2}$ (ω is the frequency of the signal) and $B_d(z^{-1})$ depends on the phase and the magnitude of the signal. Note that the term $A_d(z^{-1})$ is the *internal model* of the signal.

The narrow-band disturbance with internal model $A_d(z^{-1})$ can be asymptotically rejected by using the internal model principle, which says that in order for the feedback control system to achieve regulation ($\lim_{n\to\infty} y(n) = 0$), it is necessary to include the factor $A_d(z^{-1})$ in the denominator of the open loop transfer function. The HDD plant does not contain the factor $A_d(z^{-1})$. So we let

$$
S(z^{-1}) = S'(z^{-1})A_d(z^{-1}) \tag{11}
$$

for some polynomial $S'(z^{-1})$, which means that Q filter must be tuned to satisfy:

$$
S'(z^{-1})A_d(z^{-1}) = S_0(z^{-1}) - z^{-d}B(z^{-1})Q(z^{-1}) \tag{12}
$$

or

$$
S_0(z^{-1}) = S'(z^{-1})A_d(z^{-1}) + z^{-d}B(z^{-1})Q(z^{-1}). \tag{13}
$$

This equation has a unique solution for $S'(z^{-1})$ and $Q(z^{-1})$, if polynomials $S_0(z^{-1})$, $A_d(z^{-1})$ and $B(z^{-1})$ are known and orders of these polynomials (n_{S_0}, n_{A_d} and n_B, respectively) satisfy:

$$n_{S_0} \le n_{A_d} + n_B + d - 1. \tag{14}$$

The order n_Q of the solution $Q(z^{-1})$ is:

$$n_Q = n_{A_d} - 1. \tag{15}$$

For the narrow-band disturbance case, $n_{A_d} = 2$. So $n_Q = 1$. Since the frequency of the narrow-band disturbance (ω in $A_d(z^{-1})$) is unknown, we cannot solve Eq. (13). Instead, the coefficients of the polynomial $Q(z^{-1})$, i.e., $q_0, \ldots, q_{n_Q}$, are adaptively tuned to incorporate the internal model of the disturbance in the controller by an adaptation algorithm, which will be described in the next section.

3. Adaptation Algorithm

Throughout this section, we assume that the transfer function of the plant $G(z^{-1})$ cascaded with the notch filters shown in Fig. 3 is given by the model $P_m(z^{-1})$ in (4). Under this assumption the block diagram in Fig. 3 is equivalent to the one in Fig. 7 with an equivalent disturbance $d'(n)$. The internal model of the disturbance $d'(n)$ is same as that of the original disturbance $d(n)$.

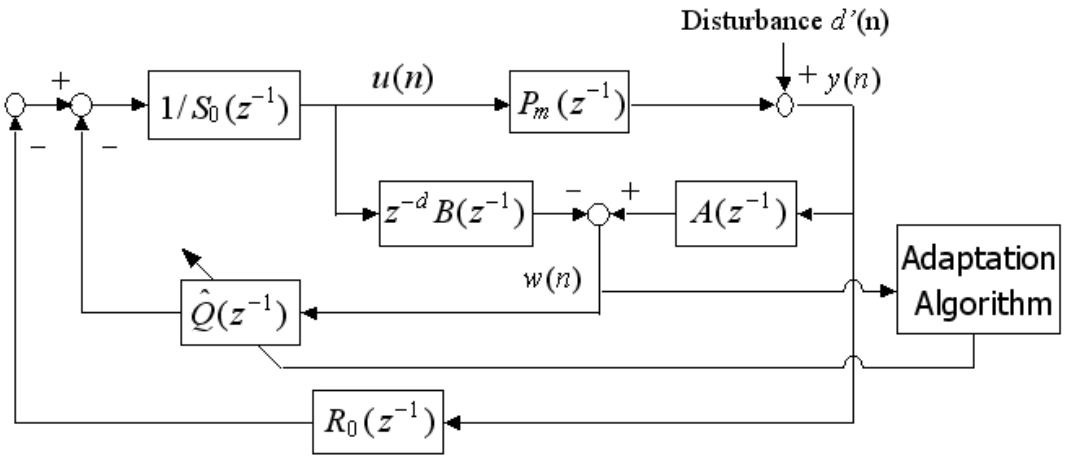

Fig. 7. Equivalent block diagram of the direct adaptive control system with accurate plant model.

Suppose we have an estimate of the Q filter at the *n*-th sample, denoted as $\hat{Q}(n, z^{-1})$ with order $n_{\hat{Q}}$. Since the objective of the present adaptive controller is to make the plant output go to zero, we define the output ($y(n)$ shown in Fig. 7) of the system with $\hat{Q}(n-1, z^{-1})$ in the presence of the disturbance as the *a priori* estimation error $\varepsilon^0(n)$, i.e.

$$\varepsilon^0(n) := y(n) = \frac{A(z^{-1})[S_0(z^{-1}) - z^{-d}B(z^{-1})\hat{Q}(n-1, z^{-1})]}{H(z^{-1})} d'(n), \tag{16}$$

where $H(z^{-1})$ is the closed-loop characteristic polynomial given by (5) and z^{-1} is interpreted as the unit sample delay operator.

As illustrated in Fig. 7, the adaptation algorithm is performed based on the signal $w(n)$, which is given by

$$w(n) = A(z^{-1})y(n) - z^{-d}B(z^{-1})u(n). \tag{17}$$

Since

$$y(n) = P_m(z^{-1})u(n) + d'(n) = \frac{z^{-d}B(z^{-1})}{A(z^{-1})}u(n) + d'(n), \tag{18}$$

we have

$$w(n) = A(z^{-1})d'(n)\,. \tag{19}$$

From (19) and (16), the *a priori* estimation error is computed by

$$\begin{aligned}\varepsilon^0(n) &= \frac{S_0(z^{-1})}{H(z^{-1})}w(n) - \hat{Q}(n-1,z^{-1})\frac{z^{-d}B(z^{-1})}{H(z^{-1})}w(n)\\ &= w_1(n) - \hat{Q}(n-1,z^{-1})w_2(n)\end{aligned}, \tag{20}$$

where

$$w_1(n) = \frac{S_0(z^{-1})}{H(z^{-1})}w(n)\,, \tag{21}$$

$$w_2(n) := \frac{z^{-d}B(z^{-1})}{H(z^{-1})}w(n)\,. \tag{22}$$

Plugging (13) into (20), we can rewrite $\varepsilon^0(n)$ as

$$\varepsilon^0(n) = [Q(z^{-1}) - \hat{Q}(n-1,z^{-1})]w_2(n) + v(n)\,, \tag{23}$$

where

$$v(n) = \frac{S'(z^{-1})A_d(z^{-1})}{H(z^{-1})}w(n) = \frac{S'(z^{-1})A_d(z^{-1})A(z^{-1})}{H(z^{-1})}d'(n)\,. \tag{24}$$

$v(n)$ asymptotically tends to zero, since $A_d(z^{-1})$ is the internal model of $d'(n)$ and $H(z^{-1})$ is stable.

Suppose that we know the order of the Q polynomial (or Q filter), i.e., $n_{\hat{Q}} = n_Q$. Define the estimated polynomial as $\hat{Q}(n,z^{-1}) = \hat{q}_0(n) + \hat{q}_1(n)z^{-1} + \cdots + \hat{q}_{n_Q}(n)z^{-n_Q}$ and the estimated parameter vector as $\hat{\theta}(n) = [\hat{q}_0(n)\ \hat{q}_1(n)\ \cdots\ \hat{q}_{n_Q}(n)]^T$. The true value of the parameter vector is $\theta = [q_0\ \ q_1\ \cdots\ q_{n_Q}]^T$ according to the definition of $Q(z^{-1})$ in (8). Also define an observation vector:

$$\phi^T(n-1) = [w_2(n)\ \ w_2(n-1)\ \cdots\ w_2(n-n_Q)]\,. \tag{25}$$

With these definitions, Eq. (23) becomes

$$\varepsilon^0(n) = [\theta - \hat{\theta}(n-1)]^T \phi(n-1) + v(n). \tag{26}$$

Equation (24) shows that $\varepsilon^0(n)$ corresponds an adaptation error as $v(n)$ tends to zero.

The adaptation algorithm to estimate the parameters of the Q polynomial is:

$$\hat{\theta}(n) = \hat{\theta}(n-1) + \frac{F(n-1)\phi(n-1)\varepsilon^0(n)}{1+\phi^T(n-1)F(n-1)\phi(n-1)}, \tag{27}$$

$$F(n) = F(n-1) - \frac{F(n-1)\phi(n-1)\phi^T(n-1)F(n-1)}{1+\phi^T(n-1)F(n-1)\phi(n-1)}. \tag{28}$$

Note that the controller parameter vector $\hat{\theta}(n)$ is updated by Eq. (27). Thus, the present adaptive controller is a direct adaptive controller.

At each sample of the operation of direct adaptive control, the signals $w_1(n)$ and $w_2(n)$ are first computed from the signal $w(n)$ according to equations (21) and (22). Then we compute the estimation error $\varepsilon^0(n)$ and update the estimated vector $\hat{\theta}(n)$ according to (27) and (28). The output of the Q filter is then computed by $\hat{Q}(n, z^{-1})w(n)$ and is applied to the servo loop as illustrated in Fig. 7.

It was proven in [9] that $\hat{\theta}(n)$ converges to θ under the following assumptions:

(i) The plant model $P_m(z^{-1}) = \dfrac{z^{-d}B(z^{-1})}{A(z^{-1})}$ is identical to the actual plant;

(ii) The model of the disturbance has poles on the unit circle (which is the case for the narrow-band disturbance);

(iii) The order n_{A_d} of the internal model of the disturbance is known, which means n_Q is known.

4. Simulation results of the direct adaptive control

To see the performance of the direct adaptive control scheme described in the previous section, the plant model given by (2) is used as the actual plant to satisfy the first assumption for the convergence of $\hat{\theta}(n)$. The baseline controller is described in Section 2. The disturbance source, including disk flutter, RRO, sensor noise, and torque noise, available in [11] is used as the baseline disturbance. A fictitious sinusoidal signal (shown in Fig. 8) at 600Hz with fast time-varying magnitude and phase depicted in Fig. 9(a) and (b) respectively is injected to the servo loop at the beginning of the third revolution to represent the narrow-band disturbance. The PES under the influence of both the baseline disturbance and the narrow-band disturbance are shown in Fig. 10.

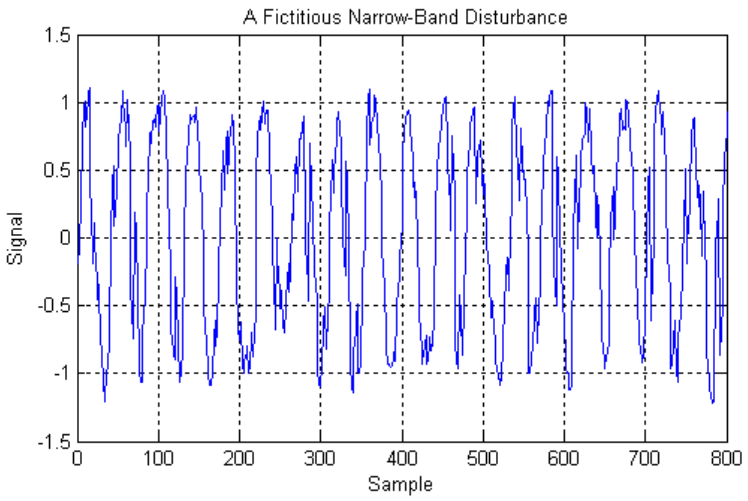

Fig. 8 Time trace of a fictitious narrow-band disturbance used in the simulation.

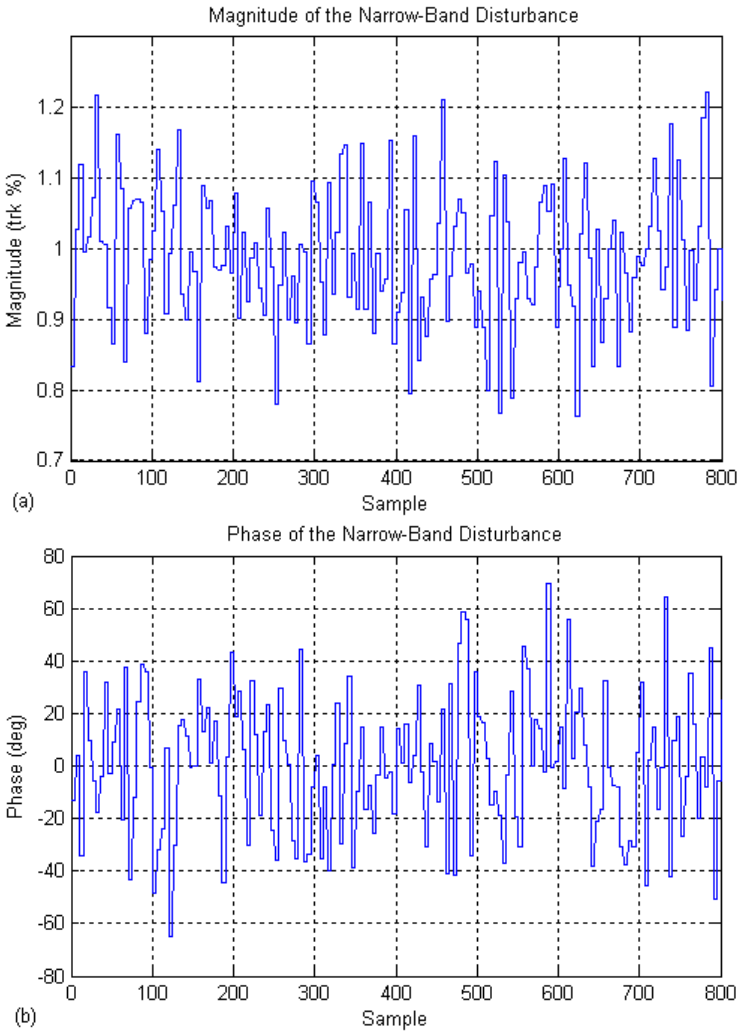

Fig. 9 Time-varying (a) magnitude and (b) phase of the narrow-band disturbance.

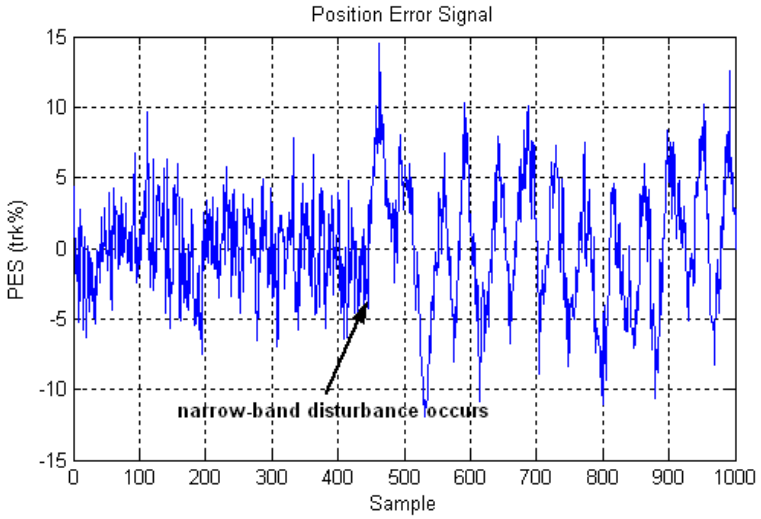

Fig. 10 The position error signal (PES) under the influence of the disturbances.

Since large narrow-band disturbances do not always occur in HDD system, the direct adaptive

controller is not activated until a large disturbance is detected, which is accomplished by monitoring the standard deviation σ of PES in a time window of one revolution (220 samples). If the 3σ value of PES (which is called TMR as mentioned in Section 1) in any one revolution is larger than a predetermined threshold (12% of the track pitch in our simulation), the estimation of the parameters of the Q polynomial as introduced in Section 3 is initiated and the estimated Q filter is applied to the servo loop in Fig. 3; otherwise, the baseline controller is used as the servo controller.

In the simulation, the TMR in the first and the second revolution is 8.52% and 8.34% of the track pitch respectively, while in the third revolution the TMR becomes 15.58% of the track pitch due to the presence of the narrow-band disturbance. Thus, the estimation of the Q polynomial starts at the beginning of the fourth revolution. Since we have one narrow-band disturbance, the order of the internal model of this disturbance is two and the order of the Q polynomial is one. Thus, there are two parameters q_0 and q_1 to estimate. Figure 11 shows the evolution of the estimates of these two parameters. Note that they converge within 50 samples. The time domain simulation result is shown in Fig. 12(a) and (b). The PES is reduced by the proposed compensation scheme (the direct adaptive control scheme) at the steady state as shown in Fig. 12(b) compared with the no compensation case (when the baseline controller is used for all the time), but due to the switch of servo controller from the baseline controller to the controller with Q filter, a big oscillation occurs when the direct adaptive controller is activated as shown in Fig. 12(a). This oscillation is handled by properly modifying the Q filter as described in the next section.

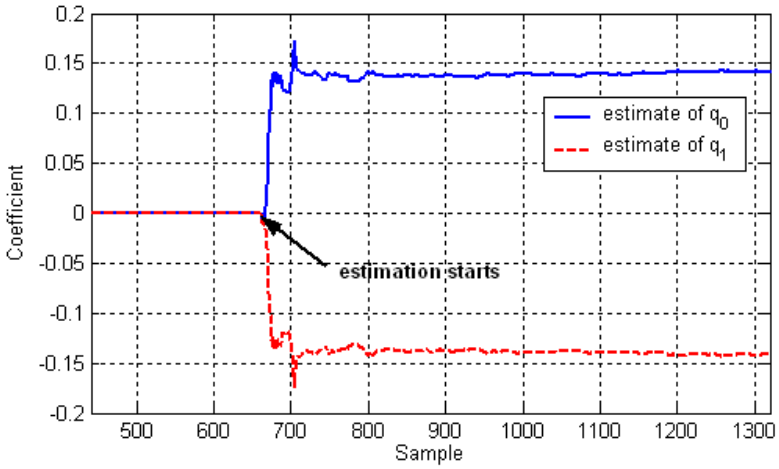

Fig. 11 Estimation of the parameters of the Q filter

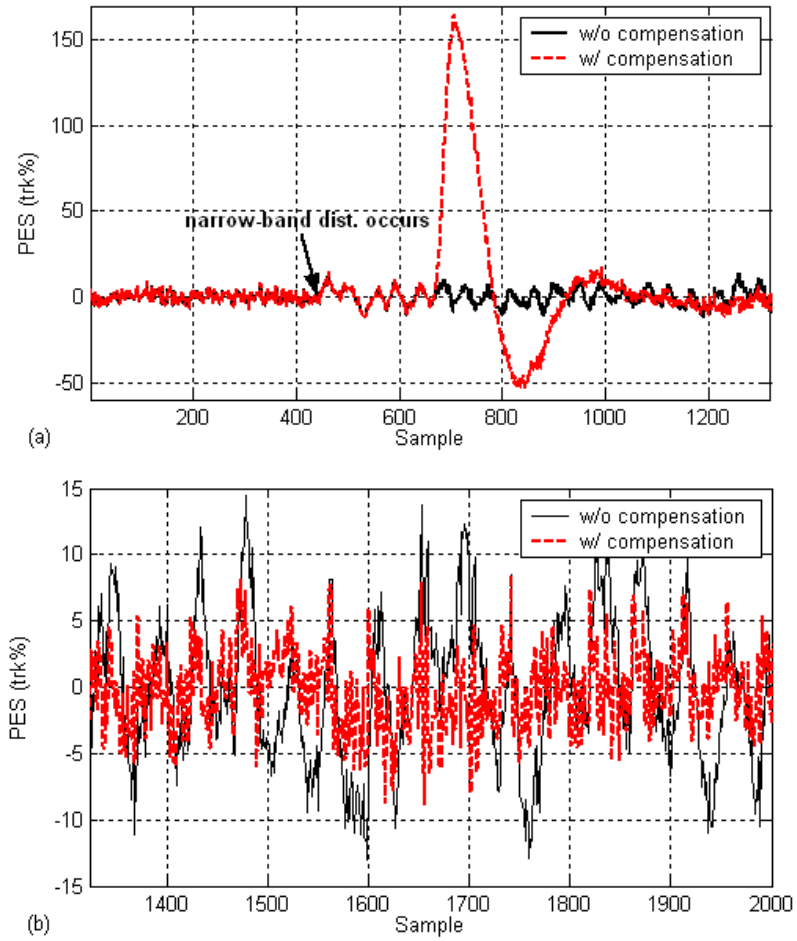

Fig. 12 Time trace of the PES: (a) in the first 6 revolutions; (b) at the steady state.

5. Direct adaptive control with modified Q filters

The simulation result in Fig. 12(a) shows a large oscillation at low frequency when the adaptive controller is activated. The baseline PID controller contains the term $1-z^{-1}$ in the denominator $S_0(z^{-1})$, which provides an infinite open-loop gain at 0Hz to reject low frequency disturbances, but the resulting controller with Q filter no longer contains this term in $S(z^{-1})$. If $Q(z^{-1})$ contains the term $1-z^{-1}$, $S(z^{-1})$ given by Eq. (7) will also incorporate this term and it turns out that the transient oscillation may be eliminated. Thus, we let

$$Q(z^{-1}) = H_S(z^{-1})Q'(z^{-1}), \tag{29}$$

where $H_S(z^{-1}) := 1-z^{-1}$ is the pre-specified term in $Q(z^{-1})$, and

$$S_0(z^{-1}) = H_S(z^{-1})S_0'(z^{-1}). \tag{30}$$

Thus, the denominator of the resulting controller becomes

$$S(z^{-1}) = H_S(z^{-1})S_0'(z^{-1}) - z^{-d}B(z^{-1})H_S(z^{-1})Q'(z^{-1}) \tag{31}$$

and $S(z^{-1})$ contains $H_S(z^{-1})$. $S(z^{-1})$ must also contain $A_d(z^{-1})$ according to the internal model principle. Therefore,

$$S(z^{-1}) = H_S(z^{-1})A_d(z^{-1})S'(z^{-1}). \tag{32}$$

Then the equation for computing the Q polynomial becomes

$$S_0'(z^{-1}) = A_d(z^{-1})S'(z^{-1}) + z^{-d}B(z^{-1})Q'(z^{-1}), \tag{33}$$

which has the unique solutions for $S'(z^{-1})$ and $Q'(z^{-1})$, if

$$n_{S_0'} \le n_{A_d} + n_B + d - 1, \tag{34}$$

where $n_{S_0'}$ is the order of $S_0'(z^{-1})$. This condition is satisfied in the present problem. The solution $Q'(z^{-1})$ has order $n_{Q'} = n_{A_d} - 1$, and the objective of our adaptation algorithm is to find the coefficients of $Q'(z^{-1})$ ($Q'(z^{-1}) = q_0' + q_1' z^{-1} + \cdots + q_{n_{Q'}}' z^{-n_{Q'}}$).

Following the procedure similar to the one in Section 3, we obtain the following updating law for estimating $\theta = [q_0' \cdots q_{n_{Q'}}']^T$:

$$\hat{\theta}(n) = \hat{\theta}(n-1) + \frac{F(n-1)\phi(n-1)\varepsilon^0(n)}{1 + \phi^T(n-1)F(n-1)\phi(n-1)}, \tag{35}$$

$$F(n) = F(n-1) - \frac{F(n-1)\phi(n-1)\phi^T(n-1)F(n-1)}{1 + \phi^T(n-1)F(n-1)\phi(n-1)}, \tag{36}$$

where

$$\varepsilon^0(n) = w_1(n) - \hat{Q}'(n-1, z^{-1}) w_2(n), \tag{37}$$

$$\hat{Q}'(n-1, z^{-1}) = \hat{q}_0'(n-1) + \hat{q}_1'(n-1) z^{-1} + \cdots + \hat{q}_{n_{Q'}}'(n-1) z^{-n_{Q'}}, \tag{38}$$

$$w_1(n) = \frac{S_0(z^{-1})}{H(z^{-1})} w(n), \tag{39}$$

$$w_2(n) = \frac{z^{-d} B(z^{-1})}{H(z^{-1})} H_S(z^{-1}) w(n), \tag{40}$$

$$\hat{\theta}(n-1) = [\hat{q}_0'(n-1) \ \cdots \ \hat{q}_{n_{Q'}}'(n-1)]^T, \tag{41}$$

$$\phi(n-1) = [w_2(n) \ \ w_2(n-1) \ \cdots \ \ w_2(n-n_{Q'})]^T. \tag{42}$$

The signal fed back to the servo loop from the Q filter is $-\hat{Q}'(n, z^{-1}) H_S(z^{-1}) w(n)$. The direct adaptive control scheme with pre-specified term in Q filter can be implemented as shown Fig. 13, after pulling out the $H_S(z^{-1})$ term from the Q filter loop.

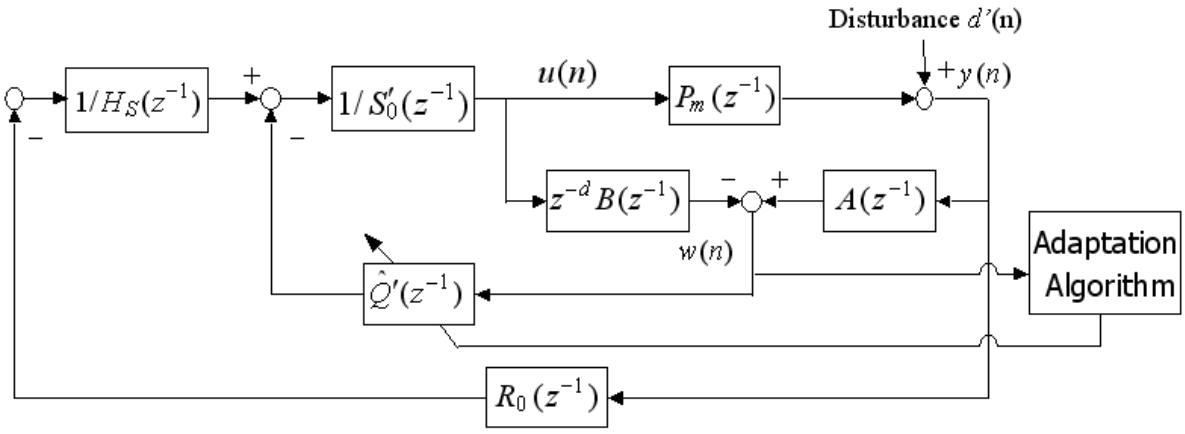

Fig. 13 Structure of the direct adaptive control with the pre-specified term in Q.

The direct adaptive control scheme with the pre-specified term in the Q filter was simulated under the same condition as in Section 4. Figure 14 shows the time trace of PES with and without compensation. It is clear that the PES is reduced by the proposed control scheme and that the low frequency oscillation does not occur in this case. Figure 15 shows the spectrum of PES after the direct adaptive control has been activated and compares it with the one without compensation. As can be seen in the figure, PES is attenuated below 1500Hz, while it is amplified in [3000Hz, 9000Hz] due to the waterbed effect. The attenuation of PES at low frequencies results in a significant reduction of the TMR (15.35% to 8.41% of the track pitch).

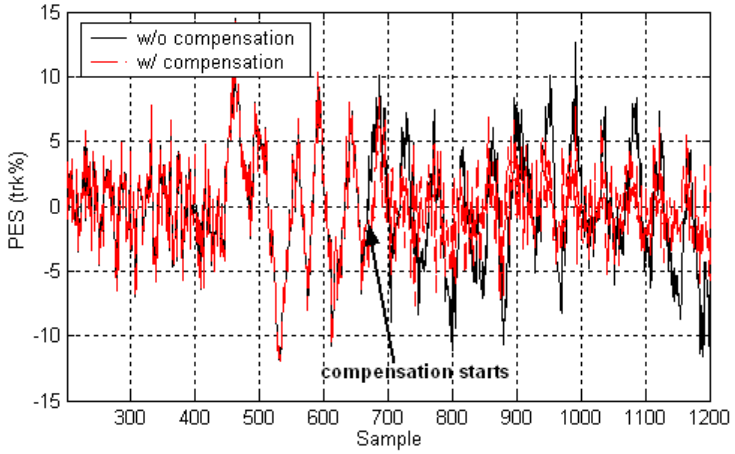

Fig. 14 Time trace of the PES with and without the direct adaptive control containing the pre-specified term.

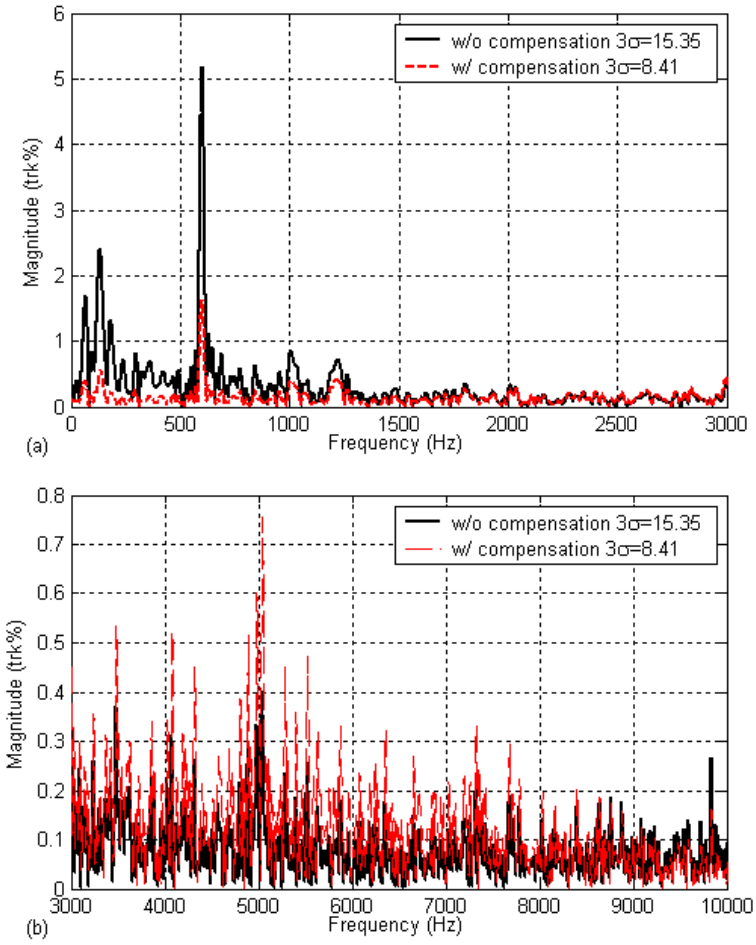

Fig. 15 Spectrum of the PES with and without compensation (pre-specified term): (a) below 3000Hz; (b) in [3000Hz, 10000Hz].

The adaptive control scheme with or without the pre-specified term in the Q filter does not work if the more realistic full model in Section 2 is used as the plant. Moreover, it is always desired that the waterbed effect is limited to a certain frequency range when we add some new dynamics to the servo controller. Notice that the frequency response of the plant model is almost the same as the full model in [200Hz, 800Hz] as shown in Fig. 6 and it is reasonable to assume that the narrow-band disturbance only happens in this frequency range. We cascade a bandpass filter $H_{BPF}(z^{-1})$ with a pass band [200Hz, 800Hz] as depicted in Fig. 16 to the Q filter. Then the Q filter is given by

$$Q(z^{-1}) = H_{BPF}(z^{-1})H_S(z^{-1})Q''(z^{-1}). \tag{43}$$

The order of $Q''(z^{-1})$ is $n_{Q''} = n_{A_d} - 1$. $Q(z^{-1}) \approx 0$ at frequencies other than [200Hz, 800Hz]. Thus, $R(z^{-1})/S(z^{-1})$ differs from $R_0(z^{-1})/S_0(z^{-1})$ only in [200Hz, 800Hz], which means that the waterbed effect caused by the Q filter containing $H_{BPF}(z^{-1})$ is limited to the pass band of $H_{BPF}(z^{-1})$.

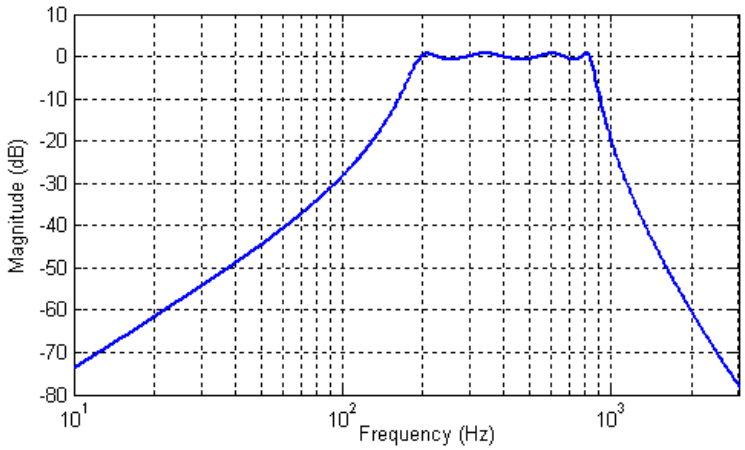

Fig. 16 Frequency response of the bandpass filter $H_{BPF}(z^{-1})$.

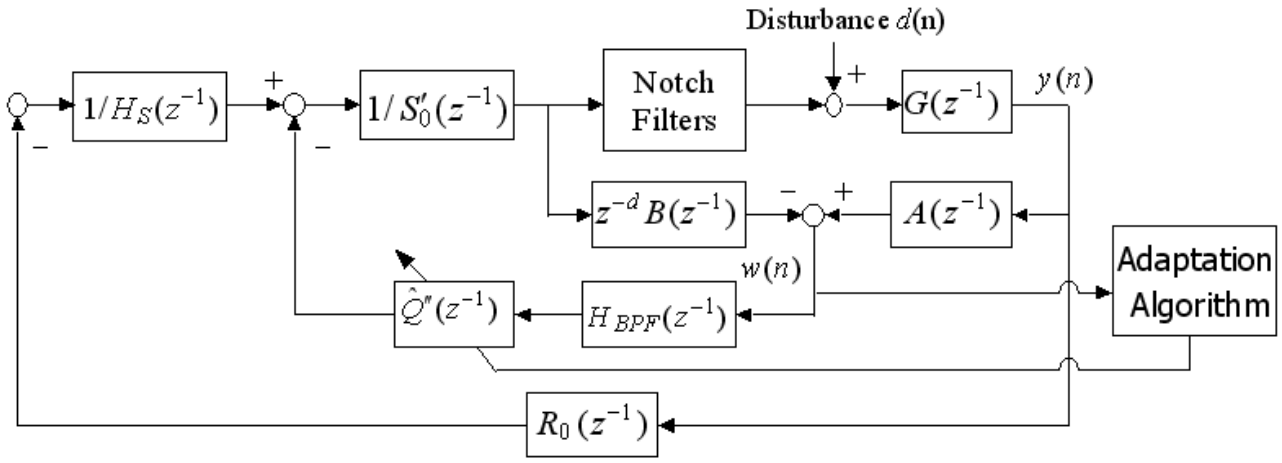

Fig. 17 Structure of the direct adaptive control with the pre-specified term and the bandpass filter in Q.

This modified direct adaptive control scheme is implemented as shown in Fig. 17. The same adaptation algorithm described by (35)-(42) is used for estimating the parameters of $Q''(z^{-1})$ except that $\hat{\theta}(n)$ is a vector of estimated parameters of $Q''(z^{-1})$ and the signal $w_2(n)$ is given

$$w_2(n) = \frac{z^{-d}B(z^{-1})}{H(z^{-1})} H_S(z^{-1}) H_{BPF}(z^{-1}) w(n). \tag{44}$$

The direct adaptive control scheme with the pre-specified term and the bandpass filter in the Q fitler works even when the full model is used to represent the HDD dynamics. Figure 18 shows the time trace of PES with and without this compensation scheme. Similar to the previous case, no low frequency oscillation happens when the adaptive controller is activated and the PES is reduced by this compensation scheme. From the spectrum of PES shown in Fig. 19, we can see that the narrow-band disturbance at 600Hz is greatly attenuated by the adaptive controller and the waterbed effect happens only in the frequency range [200Hz, 800Hz]. The TMR is reduced from 16.24% of the track pitch to 12.76% by the proposed adaptive controller.

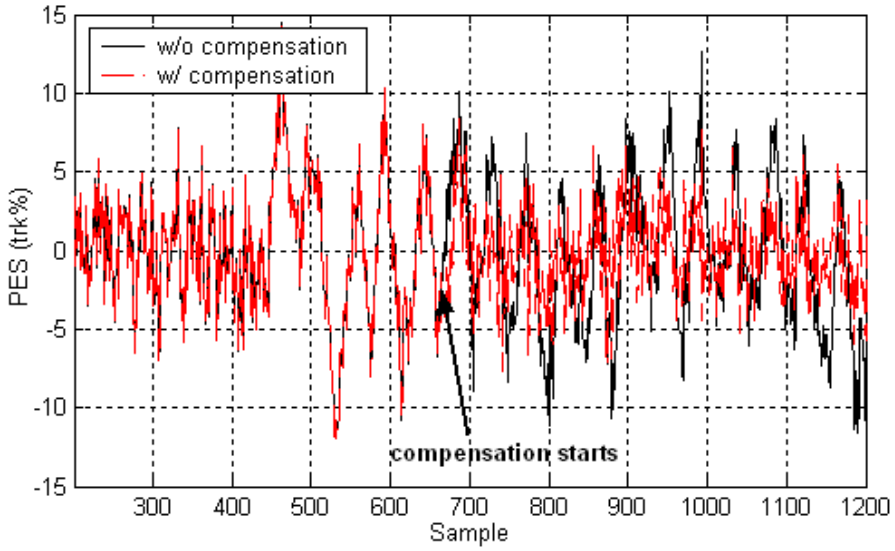

Fig. 18 Time trace of the PES with and without the direct adaptive control containing the pre-specified term the bandpass filter.

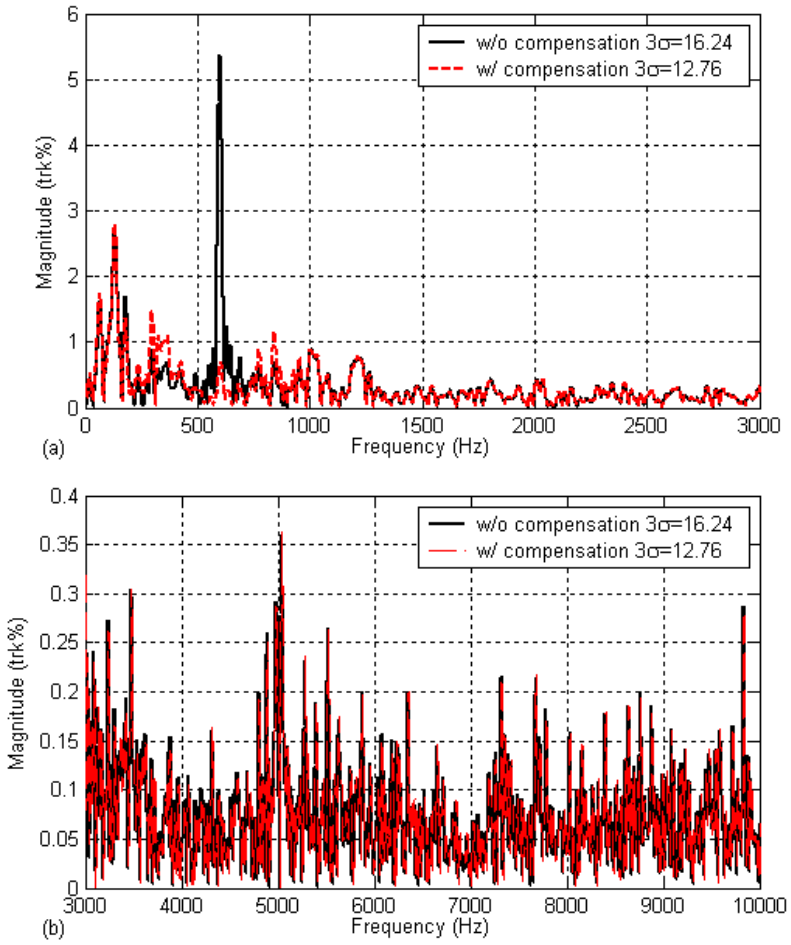

Fig. 19 Spectrum of the PES with and without compensation (pre-specified term and bandpass filter): (a) below 3000Hz; (b) in [3000Hz, 10000Hz].

6. Conclusion

This report described a direct adaptive control scheme for rejecting the narrow-band disturbances in HDDs. A stabilizing servo controller with Q filter (or Q polynomial) was built around the baseline controller based on the Youla-Kucera parameterization. The rejection of the disturbance was achieved by adaptively tuning the parameters of the Q filter so that the internal model of the disturbance presents in the controller. The adaptation algorithm was designed by minimizing the output of the HDD system with the estimated Q filter. Simulations performed using a realistic open-

source HDD simulation tool showed the fast convergence of the estimated parameters in the case of accurate plant model. A pre-specified term was then added to the Q filter to reject the large oscillation that occurred when the adaptive controller was activated. A bandpass filter was also cascaded with the Q filter to make the proposed control scheme work for the full model plant and to limit the waterbed effect to the frequency range [200Hz, 800Hz].

Acknowledgement

This work was supported by the *Computer Mechanics Laboratory of the University of California, Berkeley*.

References

[1] C. Kempf, W. Messner, M. Tomizuka and R. Horowitz, "Comparison of four discrete-time repetitive control algorithms," *IEEE Control System Magazine*, vol. 13, no. 6, pp. 48-54, Dec. 1993.

[2] S. Wu and M. Tomizuka, "Repeatable runout compensation for hard disk drives using adaptive feedforward cancellation," in *2006 American Control Conference*, pp. 6, Piscataway, NJ, USA.

[3] G. Jang, S. Hong, D. Kim, and J. Han, "New design of a HDD spindle motor using damping material to reduce NRRO," *IEEE Transactions on Magnetics*, vol.36, no.5, pp. 2258-60, Sept. 2000.

[4] D. Wu, G. Guo, and T.C. Chong, "Midfrequency disturbance suppression via micro-actuator in dual-stage HDDs," *IEEE Transactions on Magnetics*, vol.38, no.5, pp. 2189-91, Sept. 2002.

[5] M. Kobayashi, S. Nakagawa, and S. Nakamura, "A phase-stabilized servo controller for dual-stage actuators in hard disk drives," *IEEE Transactions on Magnetics*, vol. 39, no. 2, pp. 844-850, Mar. 2003.

[6] J. Zheng, G. Guo, Y. Wang, and W. Wong, "Optimal narrow-band disturbance filter for PZT-actuated head positioning control on a spinstand," *IEEE Transactions on Magnetics*, vol. 42, no. 11, pp. 3745-51, Nov. 2006.

[7] Y. Kim, C. Kang, and M. Tomizuka, "Adaptive and optimal rejection of non-repeatable disturbance in hard disk drives," in *2005 IEEE/ASME International Conference on Advanced Intelligent Mechatronics*, Monterey, vol. 1, pp. 1-6, Jul. 2005.

[8] Q. Zheng and M. Tomizuka, "Adaptive compensation of dominant frequency components of non-repeatable runout in hard disk drives," *CML Technical Report*, 06-015, Jan 2007.

[9] I.D. Landau, A. Constantinescu, and D. Rey, "Adaptive narrow band disturbance rejection applied to an active suspension – an internal model principle approach," *Automatica*, 41(4):563-574, 2005.

[10] A. Mamun, G. Guo, and C. Bi, *Hard Disk Drive: Mechatronics and Control*. Boca Raton, FL: CRC Press, 2007.

[11] M. Hirata et al. Benchmark problem of Hard Disk Drive System. http://mizugaki.iis.u-tokyo.ac.jp:80/nss/MSS_bench_e.htm.